Dilution of Precision in Positioning Systems Using Both Angle of Arrival and Time of Arrival Measurements

Article *in* IEEE Access · January 2020

DOI: 10.1109/ACCESS.2020.3033281

CITATIONS
19

READS
766

3 authors, including:

Binghao Li
UNSW Sydney
143 PUBLICATIONS **3,245** CITATIONS

SEE PROFILE

Kai Zhao
UNSW Sydney
7 PUBLICATIONS **159** CITATIONS

SEE PROFILE

IEEE Access
Multidisciplinary | Rapid Review | Open Access Journal

Received September 27, 2020, accepted October 13, 2020, date of publication October 23, 2020, date of current version November 2, 2020.

Digital Object Identifier 10.1109/ACCESS.2020.3033281

Dilution of Precision in Positioning Systems Using Both Angle of Arrival and Time of Arrival Measurements

BINGHAO LI[1], (Member, IEEE), KAI ZHAO[1], AND XUESONG SHEN[2]
[1]School of Minerals and Energy Resources Engineering, UNSW Sydney, Sydney, NSW 2052, Australia
[2]School of Civil and Environmental Engineering, UNSW Sydney, Sydney, NSW 2052, Australia

Corresponding author: Binghao Li (binghao.Li@unsw.edu.au)

ABSTRACT Dilution of precision (DOP) is a value that can describe the effect on the relationship between measurement error and position determination error. The DOP of a positioning system using time of arrival (TOA) measurement such as GPS has been well researched. Some researchers have also investigated the DOP of the angle of arrival (AOA) system. However, the DOP of the AOA and TOA combined system has been rarely studied. As more AOA based systems appear in the market, the AOA/TOA combined system is likely to be used widely in the future. This article investigates the DOP of a positioning system combining AOA and TOA. The concept of DOP is briefly introduced, and the DOP of AOA and of TOA is discussed separately. A unified formula to calculate DOP is derived for a positioning system using AOA and/or TOA measurements. The simulation shows that the DOP value is associated with the size of the deployment of the base stations and the ratio between the standard deviations of TOA and AOA measurements. If the ratio is fixed, when the size approaches infinity, the DOP approaches that of a positioning system using only TOA measurement. On the contrary, when the size approaches infinitely small, the DOP approaches that of a positioning system using only AOA measurement. An Ultra-Wide band positioning system was used to conduct experiments. The results verify that the unified formula can be used to guide the deployment of base stations of the AOA and/or TOA based positioning system.

INDEX TERMS Angle of arrival, dilution of precision, time of arrival.

I. INTRODUCTION

There are many positioning technologies such as proximity, cell ID, fingerprinting and inertial measurement unit based techniques [1]–[3], but the most popular positioning technologies are angle based or range based [4]–[11]. The angle based system measures the angle of arrival (AOA) and then applies triangulation to determine the position of a point. AOA is widely used in surveying (where the term is bearing), using optical technology to measure bearings [12]. Before Electronic Distance Measurement instrument appeared, measuring the angle accurately could be achieved much more easily than measuring range with high accuracy. Surveyors prefer to obtain bearings rather than distance to estimate position if the target is relatively further away. For AOA based radio frequency positioning systems, there are two advantages: no synchronization of the base stations is required and fewer base stations are needed. However, as an antenna array is required, the system is more complicated and difficult to install. Researchers have investigated accurate ways to estimate angle measurements [13], [14], but a modern AOA based positioning system is still rare [15]–[17]. In early 2019, Bluetooth Special Interest Group announced Bluetooth 5.1. The new specification offers AOA and Angle of Departure (AOD) for positioning [18]. A new combined time of arrival (TOA) and AOA positioning system is expected soon.

With the development of ranging technology, range based positioning systems dominate positioning applications. The most famous positioning system is GPS which uses TOA to estimate the receiver's position [4]. All the satellite based positioning systems use TOA. Before the era of global navigation satellite systems, Time Difference of Arrival (TDOA) was applied in many positioning systems such as Loran-C

The associate editor coordinating the review of this manuscript and approving it for publication was Venkata Ratnam Devanaboyina.

and Omega [5], [19]. Recent examples of the terrestrial positioning and navigation systems are cellular phone networks [6], Locata [7] and Ultra-Wide band (UWB) [20].

For a range or angle measurement based positioning system, the geometric distribution of the base stations affects the positioning accuracy [21]. Dilution of precision (DOP) is used to describe the effect on the relationship between measurement error and position determination error. DOP has been well investigated for range based positioning systems, especially global navigation satellite systems [4], [21]–[24], and DOP for angle based systems has also been discussed in recent studies [25], [26]. The introduction of Bluetooth 5.1 shows that we may use AOA more in the new positioning system and a combination of AOA and TOA may be commonly used. The Cramer-Rao Bound (CRB) of a hybrid positioning system in a 2D scenario was derived in [27] to analyze the theoretical performance limits. In comparison, DOP is a more convenient index which can help optimize the geometric distribution of the base stations.

The main contribution of this research is deriving a unified formula to calculate DOP for a positioning system using AOA and/or TOA measurements for the first time. Simulation was used to understand the features of the DOP of the combined system. The unified formula can be used to guide the deployment of base stations of the AOA and/or TOA based positioning system and has been confirmed by experiments.

The concept of DOP is explained in section II, and then the theoretical issues of DOP for AOA and TOA are reviewed in section III. In section IV, the DOP for the AOA and TOA combined system is discussed. Simulations carried out to investigate the deployment of the base stations are introduced in section V, followed by discussion of experiments using an UWB positioning system in section VI. Section VII provides a further discussion of the DOP for the AOA and TOA combined system. Finally, section VIII concludes.

II. CONCEPT OF DOP

Geometric DOP (GDOP) is used to state how errors in the measurement will affect the final state estimation. Commonly, it is expressed as the ratio of the root mean square (rms) position error to the rms measurement (range or angle measurement) error [28], [29]:

$$GDOP = \frac{\sigma_p}{\sigma} \tag{1}$$

Obviously, a smaller DOP is preferred. A small DOP means small changes in the measurement will not result in large errors in the location output. Fig. 1 gives several examples of GDOP when TOA, AOA and TOA/AOA are used for positioning. When TOA is used, three typical scenarios are depicted in (a)-(c). The crosses represent the base stations; the two concentric arcs indicate the range measurement error. The scenario in (a) is an example of a good DOP. The angle of intersection of the two lines which connect the

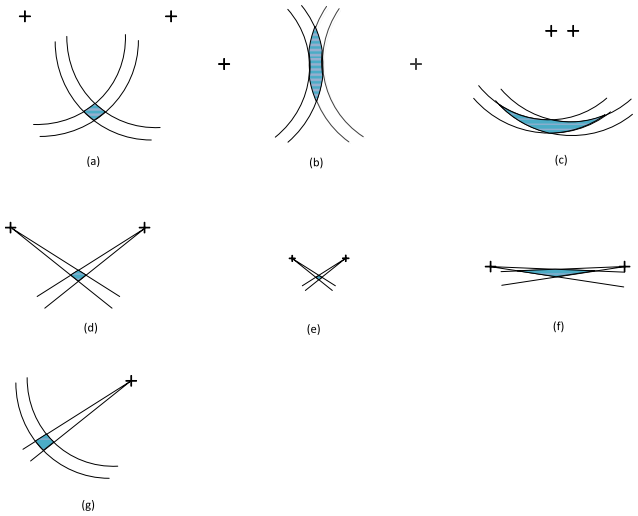

FIGURE 1. GDOP examples when TOA (a, b, c), AOA (d, e, f) and TOA/AOA (g) are used for positioning. Crosses are the base stations.

area of interest and the base stations is about 90 degrees. Plots (b) and (c) are two examples of poor DOP. Plots (d)-(f) show examples of using AOA where (d) and (e) are the same but with different scales. It indicates that the DOP for AOA is a quantity with a unit. When the distance from the base station to the mobile station increases, the AOA measurement error increases. In the TOA system, the range measurement error is always the same (in an ideal situation). Plots (e) and (g) also reveal that the DOP is poor when the positioning area is near the line that connects the two base stations, and the DOP is good when the two lines which connect the mobile station and the base stations create a right angle. Plot (g) shows that in the combined system, the DOP increases when the mobile station is further away from the base station, assuming one base station can provide both AOA and TOA measurements. DOP can be expressed as a number of separate measurements such as HDOP (horizontal DOP) and VDOP (vertical DOP) when 3D positioning is required, TDOP (time DOP) when pseudorange measurements are used, and PDOP (position DOP) which is the same as GDOP if no pseudorange measurements are used [4], [22].

III. DOPs FOR AOA AND TOA

A. AOA FOR 2D SCENARIO

In 2D AOA positioning a minimum of two base stations are required, as illustrated in Fig. 2. Assuming that the base station measures the direction of propagation of a signal (radio-frequency wave) with respect to an absolute reference (the reference direction is along the x axis in Fig. 2), it is possible to measure the AOA at the mobile station side; however the antenna array makes the size of the mobile station big. The AOA is more likely to be obtained by a base station [30]. Once the absolute angle is obtained, the angle from the mobile station to the base station can be modeled as:

$$\tan^{-1}\left(\frac{y - y_i}{x - x_i}\right) = \varphi_i \tag{2}$$

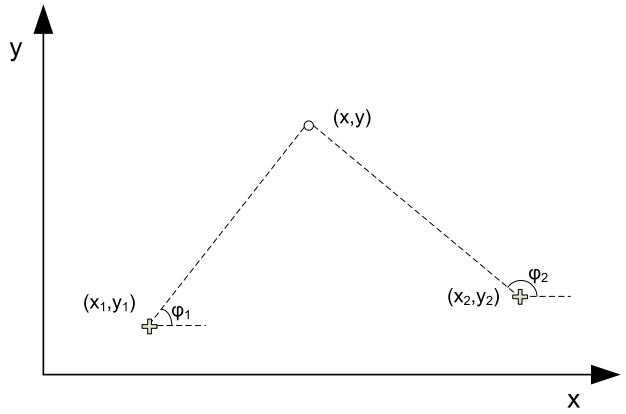

FIGURE 2. Angle measurements from a mobile station to two base stations in 2D scenarios (the reference direction is along the *x* axis).

The above equation can be expressed in a simpler form:

$$L = f(c) \tag{3}$$

where L is the direction of the signal from the mobile station to the base station, c is the coordinate of the mobile station. To linearize the equation, Taylor's theorem can be applied:

$$f(c) = f(c_0) + f'(c_0)dc + \frac{f''(c_0)(dc)^2}{2!} + \cdots + \frac{f^{(n)}(c_0)(dc)^n}{n!} + R \tag{4}$$

where R is a remainder term. By applying first order Taylor theorem on both sides of (2), we can obtain:

$$-\frac{y-y_i}{{s_i}^2}dx + \frac{x-x_i}{{s_i}^2}dy = -\tan^{-1}\frac{y-y_i}{x-x_i} + \varphi_i + d\varphi_i \tag{5}$$

where

$$s_i = \sqrt{(x-x_i)^2 + (y-y_i)^2} \tag{6}$$

According to (2), the sum of the constant terms is 0 and the above equations can be expressed in matrix notation:

$$AdX = db \tag{7}$$

where

$$A = \begin{bmatrix} -\frac{y-y_1}{{s_1}^2} & \frac{x-x_1}{{s_1}^2} \\ \cdots & \cdots \\ -\frac{y-y_n}{{s_n}^2} & \frac{x-x_n}{{s_n}^2} \end{bmatrix} \tag{8}$$

$$dX = \begin{bmatrix} dx \\ dy \end{bmatrix} \tag{9}$$

$$db = \begin{bmatrix} d\varphi_1 \\ \cdots \\ d\varphi_n \end{bmatrix} \tag{10}$$

It is assumed that the standard deviations of measurements from different base stations are identical:

$$\sigma_\varphi = \sigma_{\varphi_1} = \cdots = \sigma_{\varphi_n} \tag{11}$$

The various DOP quantities can be expressed as:

$$XDOP = \frac{\sqrt{{\sigma_x}^2}}{\sigma_\varphi} = \sqrt{\left((A^TA)^{-1}\right)_{1,1}} \tag{12}$$

$$YDOP = \frac{\sqrt{{\sigma_y}^2}}{\sigma_\varphi} = \sqrt{\left((A^TA)^{-1}\right)_{2,2}} \tag{13}$$

$$GDOP = \frac{\sqrt{{\sigma_p}^2}}{\sigma_\varphi} = \sqrt{trace\left((A^TA)^{-1}\right)} \tag{14}$$

where $\sigma = \sigma_\varphi$. PDOP and GDOP are identical. As the positioning result has a unit of m, the angle measurement is in radians, the DOP value has a unit of m, which has a clear meaning that 1 radian angle measurement error introduces DOP times 1 meter positioning error [26].

B. TOA FOR 2D SCENARIO

In 2D TOA positioning, at least three base stations are required. In fact, if only two base stations are available, there is ambiguity in the positioning result; the third range measurement can solve the ambiguity. The range can be modeled as:

$$r_i = \sqrt{(x-x_i)^2 + (y-y_i)^2} \tag{15}$$

The A matrix and db are:

$$A = \begin{bmatrix} \frac{x-x_1}{s_1} & \frac{y-y_1}{s_1} \\ \cdots & \cdots \\ \frac{x-x_n}{s_n} & \frac{y-y_n}{s_n} \end{bmatrix} \tag{16}$$

$$db = \begin{bmatrix} dr_1 \\ \cdots \\ dr_n \end{bmatrix} \tag{17}$$

It is assumed that the standard deviations of measurements (ranges) from different base stations are identical:

$$\sigma_r = \sigma_{r_1} = \cdots = \sigma_{r_n} \tag{18}$$

The XDOP, YDOP and GDOP can be expressed as (12)-(14), where $\sigma = \sigma_r$. For TOA systems based on absolute range measurements, PDOP and GDOP quantities are identical as there is no TDOP term [20].

C. AOA FOR 3D SCENARIOS

For 3D scenarios, AOA is slightly more complicated as there are two angle measurements available from the mobile station to each base station: an azimuth-like angle (φ_i) which is the same as in 2D scenarios, and an elevation-like angle (θ_i). Fig. 3 illustrates these two angle quantities from a mobile station (x, y, z) to a base station (x_i, y_i, z_i). The two angles can be expressed as:

$$\begin{cases} \tan^{-1}\frac{y-y_i}{x-x_i} = \varphi_i \\ \tan^{-1}\frac{s_i}{z-z_i} = \theta_i \end{cases} \tag{19}$$

where s_i is defined as (6).

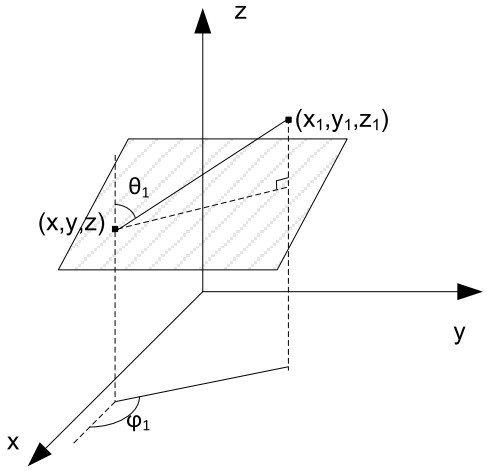

FIGURE 3. The azimuth-like angle (the reference direction is along the x axis) and the elevation-like angle (the reference direction is along the z axis) in 3D scenarios from the mobile station (x, y, z) to the base station (x_1, y_1, z_1).

For 3D positioning, still only two base stations are needed, and the corresponding A matrix is:

$$A = \begin{bmatrix} -\frac{y-y_1}{{s_1}^2} & \frac{x-x_1}{{s_1}^2} & 0 \\ \cdots & & \\ -\frac{y-y_n}{{s_n}^2} & \frac{x-x_n}{{s_n}^2} & 0 \\ \frac{(x-x_1)(z-z_1)}{{u_1}^2 s_1} & \frac{(y-y_1)(z-z_1)}{{u_1}^2 s_1} & -\frac{s_1}{{u_1}^2} \\ \cdots & & \\ \frac{(x-x_n)(z-z_n)}{{u_n}^2 s_n} & \frac{(y-y_n)(z-z_n)}{{u_n}^2 s_n} & -\frac{s_n}{{u_n}^2} \end{bmatrix} \tag{20}$$

where

$$u_i = \sqrt{(x-x_i)^2 + (y-y_i)^2 + (z-z_i)^2} \tag{21}$$

$$dX = \begin{bmatrix} dx \\ dy \\ dz \end{bmatrix} \tag{22}$$

$$db = \begin{bmatrix} d\varphi_1 \\ \cdots \\ d\varphi_n \\ d\theta_1 \\ \cdots \\ d\theta_n \end{bmatrix} \tag{23}$$

The DOPs can be expressed as (12)-(14). It is assumed that the standard deviations of angles are identical:

$$\sigma_\varphi = \sigma_{\varphi_1} = \cdots = \sigma_{\varphi_n} = \sigma_{\theta_1} = \cdots = \sigma_{\theta_n} \tag{24}$$

D. TOA FOR 3D SCENARIOS

In 3D TOA positioning, ideally at least four base stations are required, as the fourth measurement can help solve the ambiguity of the positioning result. However, in many cases, the ambiguity can be solved using other information such as above the ground [4]. The ranges can be modeled as:

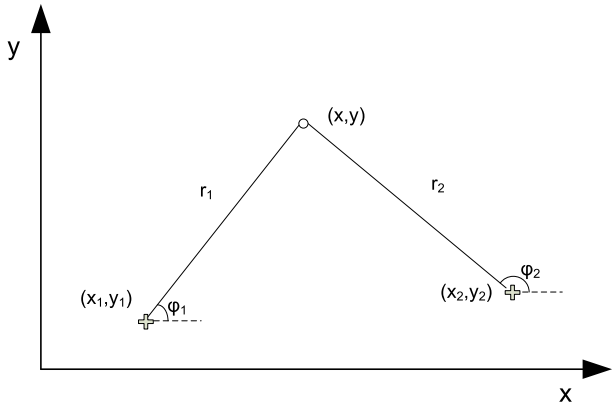

FIGURE 4. Angle and range measurements from mobile station to two base stations in 2D scenarios.

$$r_i = \sqrt{(x-x_i)^2 + (y-y_i)^2 + (z-z_i)^2} \tag{25}$$

As there is no significant difference between 3D and 2D scenarios, the details of the equations are omitted here.

IV. DOP FOR COMBINED AOA AND TOA

A. 2D SCENARIOS

Assuming each base station can have both angle and range measurements (see Fig. 4), for a 2D scenario, the following observation equations can be obtained:

$$\begin{cases} \tan^{-1}\left(\frac{y-y_i}{x-x_i}\right) = \varphi_i \\ \sqrt{(x-x_i)^2 + (y-y_i)^2} = r_i \end{cases} \tag{26}$$

The corresponding A matrix and db matrix are:

$$A = \begin{bmatrix} -\frac{y-y_1}{{s_1}^2} & \frac{x-x_1}{{s_1}^2} \\ \cdots & \cdots \\ -\frac{y-y_n}{{s_n}^2} & \frac{x-x_n}{{s_n}^2} \\ \frac{x-x_1}{s_1} & \frac{y-y_1}{s_1} \\ \cdots & \cdots \\ \frac{x-x_n}{s_n} & \frac{y-y_n}{s_n} \end{bmatrix} \tag{27}$$

$$db = \begin{bmatrix} d\varphi_1 \\ \cdots \\ d\varphi_n \\ dr_1 \\ \cdots \\ dr_n \end{bmatrix} \tag{28}$$

It is assumed that (11) and (18) exist, and there is a relationship between σ_r and σ_φ as below:

$$k = \frac{\sigma_r}{\sigma_\varphi} \tag{29}$$

Note that k has a unit of m/rad. A weight matrix can be denoted as:

$$W = \begin{bmatrix} k^2 & & & & & \\ & \cdots & & & & \\ & & k^2 & & & \\ & & & 1 & & \\ & & & & \cdots & \\ & & & & & 1 \end{bmatrix} \tag{30}$$

And the covariance of db can be expressed as:

$$cov(db) = \begin{bmatrix} \frac{1}{k^2} & & & & & \\ & \cdots & & & & \\ & & \frac{1}{k^2} & & & \\ & & & 1 & & \\ & & & & \cdots & \\ & & & & & 1 \end{bmatrix} {\sigma_r}^2 \tag{31}$$

Equation (7) can be converted to:

$$WAdx = Wdb \tag{32}$$

And the covariance matrix of the position result can be derived as follows:

$$\begin{aligned} cov(dp) &= E(dpdp^T) \\ &= E[(A^T WA)^{-1} A^T Wdbdb^T WA(A^T WA)^{-1}] \\ &= (A^T WA)^{-1} A^T Wcov(db)WA(A^T WA)^{-1} \\ &= (A^T WA)^{-1} Q \end{aligned} \tag{33}$$

where $Q = {\sigma_r}^2$. Given $cov(dp) = \begin{bmatrix} {\sigma_x}^2 & \sigma_{xy} \\ \sigma_{yx} & {\sigma_y}^2 \end{bmatrix}$, the variance of the mobile station's location can be expressed as a function of the variance of the measurements (including the angle and the range) and the geometric distribution of the base stations and the mobile station:

$$cov(dp) = F\left[\sigma_\varphi, \sigma_r, [x, y], [x_1, y_1], \cdots, [x_n, y_n]\right] \tag{34}$$

The various DOP quantities are similar to (12)-(14):

$$XDOP = \frac{\sqrt{{\sigma_x}^2}}{\sigma} = \sqrt{\left((A^T WA)^{-1}\right)_{1,1}} \tag{35}$$

$$YDOP = \frac{\sqrt{{\sigma_y}^2}}{\sigma} = \sqrt{\left((A^T WA)^{-1}\right)_{2,2}} \tag{36}$$

$$GDOP = \frac{\sqrt{{\sigma_p}^2}}{\sigma} = \sqrt{trace\left((A^T WA)^{-1}\right)} \tag{37}$$

where $\sigma = \sigma_r$. The DOP quantity here is unitless. But the DOP value is associated with the size of the deployment area of the positioning system. In A matrix, the elements in the upper part have a denominator of ${s_i}^2$. When the area scales up, the value of these elements will decrease, however, the value of the elements in the lower part of the A matrix will remain the same. This explains why the DOP quantity for the AOA base system is associated with the size (distance apart) of the deployment of the system, while the DOP quantity for the TOA base system is not.

B. 3D SCENARIOS

For 3D scenarios, if there are n base stations, for one mobile station, the total number of measurements is $3n$, including n range measurements, n azimuth-like angle measurements and n elevation-like angle measurements. The equations are:

$$\begin{cases} \tan^{-1}\dfrac{y - y_i}{x - x_i} = \varphi_i \\ \tan^{-1}\dfrac{s_i}{z - z_i} = \theta_i \\ \sqrt{(x - x_i)^2 + (y - y_i)^2 + (z - z_i)^2} = r_i \end{cases} \tag{38}$$

We assume there are coefficients k_θ and k_φ which are defined as the ratio of the standard deviations:

$$k_\varphi = \frac{\sigma_r}{\sigma_\varphi} \quad k_\theta = \frac{\sigma_r}{\sigma_\theta} \tag{39}$$

Assuming the standard deviations of θ_i and φ_i are identical, the coefficient can be denoted as:

$$k = k_\varphi = k_\theta \tag{40}$$

A, dX and db can be expressed as:

$$A = \begin{bmatrix} -\dfrac{y - y_1}{{s_1}^2} & \dfrac{x - x_1}{{s_1}^2} & 0 \\ \cdots & & \\ -\dfrac{y - y_n}{{s_n}^2} & \dfrac{x - x_n}{{s_n}^2} & 0 \\ \dfrac{(x - x_1)(z - z_1)}{{u_1}^2 s_1} & \dfrac{(y - y_1)(z - z_1)}{{u_1}^2 s_1} & -\dfrac{s_1}{{u_1}^2} \\ \cdots & & \\ \dfrac{(x - x_n)(z - z_n)}{{u_n}^2 s_n} & \dfrac{(y - y_n)(z - z_n)}{{u_n}^2 s_n} & -\dfrac{s_n}{{u_n}^2} \\ \dfrac{x - x_1}{u_1} & \dfrac{y - y_1}{u_1} & \dfrac{z - z_1}{u_1} \\ \cdots & & \\ \dfrac{x - x_n}{u_n} & \dfrac{y - y_n}{u_n} & \dfrac{z - z_n}{u_n} \end{bmatrix} \tag{41}$$

$$dX = \begin{bmatrix} dx \\ dy \\ dz \end{bmatrix} \tag{42}$$

$$db = \begin{bmatrix} d\varphi_1 \\ \cdots \\ d\varphi_n \\ d\theta_1 \\ \cdots \\ d\theta_n \\ dr_1 \\ \cdots \\ dr_n \end{bmatrix} \tag{43}$$

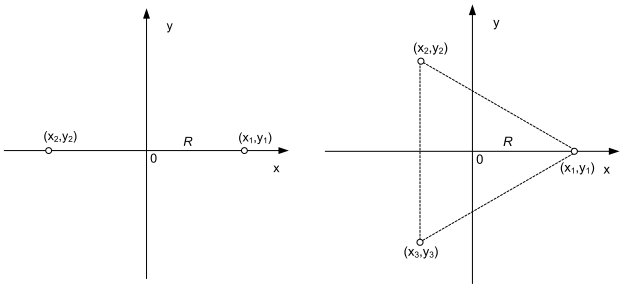

FIGURE 5. The deployment of the base stations: two base stations (left) and three base stations (right). R is the distance between the origin and a base station.

And the W matrix is:

$$W = \begin{bmatrix} k^2 & & & & & & & \\ & \cdots & & & & & & \\ & & k^2 & & & & & \\ & & & k^2 & & & & \\ & & & & \cdots & & & \\ & & & & & k^2 & & \\ & & & & & & 1 & \\ & & & & & & & \cdots \\ & & & & & & & & 1 \end{bmatrix} \quad (44)$$

The various DOP quantities are the same as (35)-(37).

V. DOP VALUES WITH DIFFERENT CONFIGURATIONS OF BASE STATIONS

In this section, we investigate the DOP values with different configurations of base stations based on Matlab simulation when an AOA/TOA combined positioning system is used.

If there is only one base station in a 2D scenario, the geometric distribution is unique. According to (27) and (37), the DOP can be calculated as below:

$$GDOP = 1 + s^2/k^2 \quad (45)$$

where k is the ratio of variances defined in (29) and s is the range between the base station and the user. This means that the DOP has a negative correlation with the distance from the base station and the station should be placed at the center of the environment to maximize the average accuracy.

In the following part, the use of two base stations and three base stations is investigated. Fig. 5 provides details of the base stations' locations. For the 3D scenario, the height of the base stations is zero unless otherwise stated.

A. 2D SCENARIO

As mentioned in previous research [22]–[25], the DOP value is irrelevant to the σ of AOA or TOA measurements in a stand-alone positioning method. However, in a hybrid positioning approach, the σ of TOA and the σ of AOA are independent from each other. The ratio of them (k defined in (40)) is a factor which can affect the DOP values.

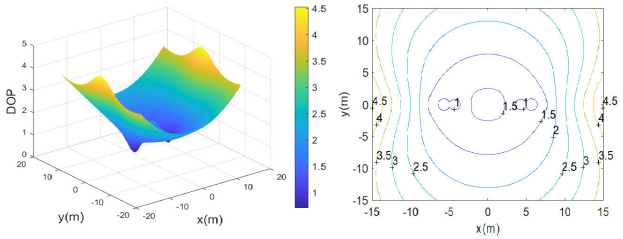

FIGURE 6. GDOP plots (mesh plot and contours) when there are two base stations and R=5m.

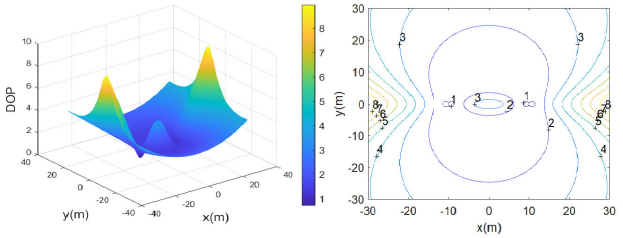

FIGURE 7. GDOP plots (mesh plot and contours) when there are two base stations and R=10m.

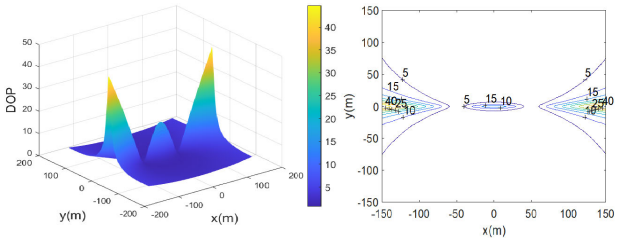

FIGURE 8. GDOP plots (mesh plot and contours) when there are two base stations and R=50m.

The accuracy of the TOA and AOA measurements can vary when different technologies are applied. In our simulation, we assume the σ of TOA is 0.1m and the σ of AOA is 0.05rad which leads to the ratio k of 2m/rad. When there are only two base stations deployed as shown in Fig. 5 (left), assuming R = 5m, the GDOP quantities are calculated in the square area centered at (0, 0) and with vertexes at ($\pm$15, $\pm$15). The results are shown in Fig. 6. The GDOP values in the areas close to the two base stations are below 1 (the best areas), and the GDOP values are also good in the area in the middle. However, the values in the center increase slightly. The GDOP increases quickly along the extension line of the two base stations' connection. As discussed previously, scaling up the deployment area will change the values of the GDOP. When R increases to 10m, generally the GDOP values increase (see Fig. 7) and the peanut shape contours are clearer. When R increases to 50m, more significant changes in the pattern can be seen (see Fig. 8).

In the case of three base stations (see Fig. 5 right for the deployment of the base stations), when the R increases from 5m to 10m and then to 50m, the changes in GDOP can be noticed, however, the changes are not as significant as when

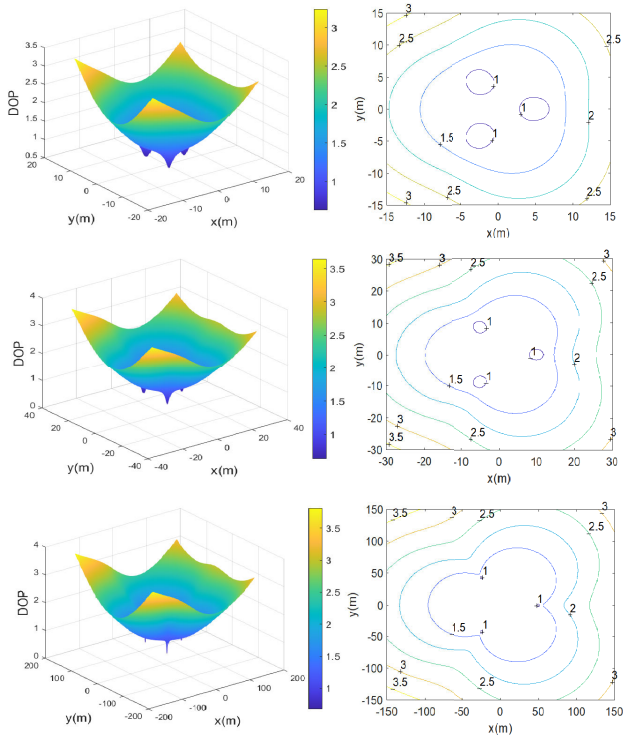

FIGURE 9. GDOP plots (mesh plot and contours) when there are three base stations (from top to bottom, R=5m, 10m, 50m).

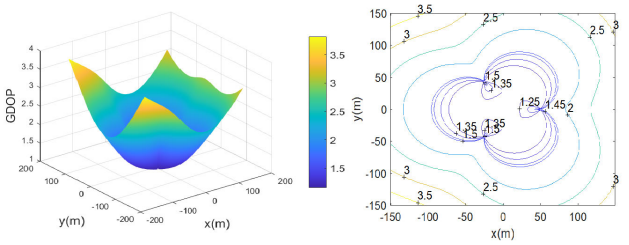

FIGURE 10. GDOP plots (mesh plot and contours) using TOA when there are three base stations.

two base stations are used (see Fig. 9). The reason is that when there are three stations, range measurements can be used to estimate the position independently. Scaling up the deployment of base stations does not affect TOA. It is a reasonable conjecture that when R tends to infinity, the GDOP tends to that of using TOA only. Fig. 10 depicts the GDOP when only TDOA is used ($R = 50$m). The plots are similar to the plots in Fig. 9. On the contrary, when R tends to 0, the GDOP tends to that of using AOA only. More details are discussed in section VII.

B. 3D SCENARIO

Assume the k is also 2m/rad. When there are three base stations as shown in Fig. 5, the GDOP quantities are calculated for various situations. The mobile station in the x-y plane with height of 0 is investigated as changing the height of the mobile station is equivalent to varying the height of the base

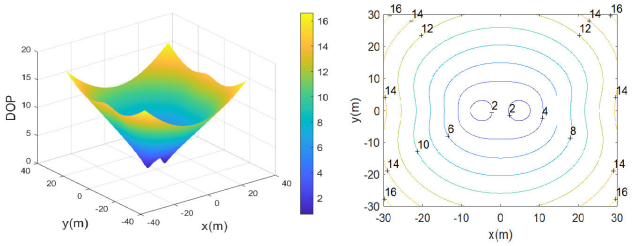

FIGURE 11. GDOP plots (mesh plot and contours) at the x-y plane with z=0 when there are two base stations, R=5m, the height of the base stations is 0m.

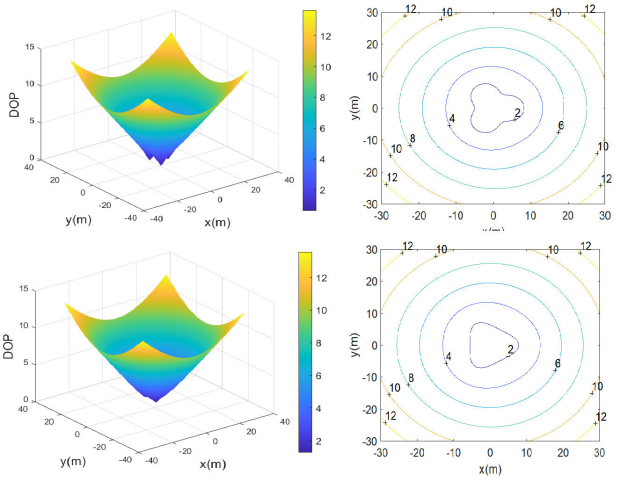

FIGURE 12. GDOP plots (mesh plot and contours) at the x-y plane with z=0 when there are three base stations, R=5m, the height of the base stations is 0m (top) and 4m (bottom).

stations. Fig. 11 shows the mesh plot and contours of GDOP when two base stations are deployed. The GDOP value is relatively high which means the positioning result will not be very good although only two base stations are enough for 3D positioning. Fig. 12 gives the GDOP when three base stations are deployed. The DOP value improved especially in the area close to the base stations or inside the triangular area surrounded by the base stations. When the height of the base stations changes from 0 to 4m, better DOP values can be obtained which means deploying the station not at the same plane for positioning will help improve the DOP. Fig. 13 is generated to compare the DOP of two different sizes of the deployment. When the size scales up, the DOP gets worse. A similar phenomenon was found in the 2D scenario. Scaling up the size means the AOA measurements are less likely to be used for positioning and we know that using TOA measurements only cannot estimate the mobile station's position if the base stations are in the same plane as the mobile station is located.

VI. EXPERIMENTS AND RESULTS

The DOP value can be used to predict the position accuracy and to guide the deployment of the base stations to achieve the best positioning results. To confirm the usefulness of the developed TOA/AOA DOP, two tests were carried out in

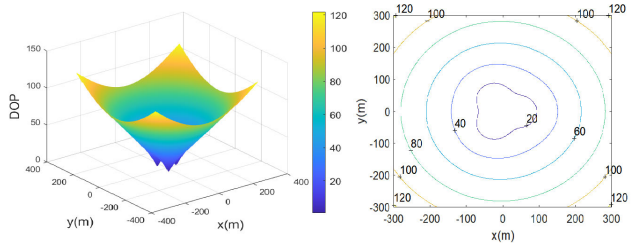

FIGURE 13. GDOP plots (mesh plot and contours) at the x-y plane with z=0 when there are three base stations, R=50m, the height of the base stations is 0m.

indoor environments. As an instrument which can provide both TOA and AOA is not available, the DW1000 radio IC [31] based UWB positioning system was used to provide the TOA measurement, and the AOA measurements were simulated.

Fig. 14 shows a base station and a mobile station of a UWB positioning system developed by the authors for the experiment. The UWB system was set to work on 3993.6MHz with a bandwidth of 499.2MHz. UWB can minimize the multipath effect and produce centimeter-level range measurements. The σ of TOA measurements is 2.14cm, which is calculated based on the samples collected in the same experimental environment. The σ of AOA was set to 0.0107rad, which ensures the k is consistent with its own value in section V. The configurations of the two tests are shown in Fig. 15. Note that these tests are used to verify the developed DOP, and it does not matter if the base stations are deployed at the optimized location. The plot at the top of Fig. 15 gives the coordinates of the base stations and mobile station; the photos at the bottom of Fig. 15 show the test environments. At each test point, at least 300 TOA measurements were obtained.

Figures 16 and 17 show the positioning results. In the case of two base stations, if only TOA measurements are available, 2D positioning is possible, however, the DOP value is large [28]. If the base station is located exactly along the line connecting (x_1, y_1) and (x_2, y_2), the DOP value is infinity. When the test was carried out, the base stations and the mobile station could not be located exactly at the planned location. The 2D position of the mobile station could still be estimated, but the accuracy was poor as the DOP indicated. As expected, the positioning errors decreased when the mobile station moved toward (x_1, y_1) and then increased quickly when the mobile station moved away from (x_1, y_1) (see Fig. 16 left). When TOA and AOA measurements were all used, it is very clear that the positioning errors are much smaller, and the change of the error is in line with expectations (see Fig. 6 and Fig. 16 right). It can also be noted that the error in the y direction is significantly larger than in the x direction which can also be explained by the geometric distribution of the base stations in the x or y direction. When 3D positioning is required, at least three base stations are needed when only TOA is applied. Fig. 17 (left) shows the results. When the mobile station is further away from the

FIGURE 14. UWB base station (left) and mobile station (right).

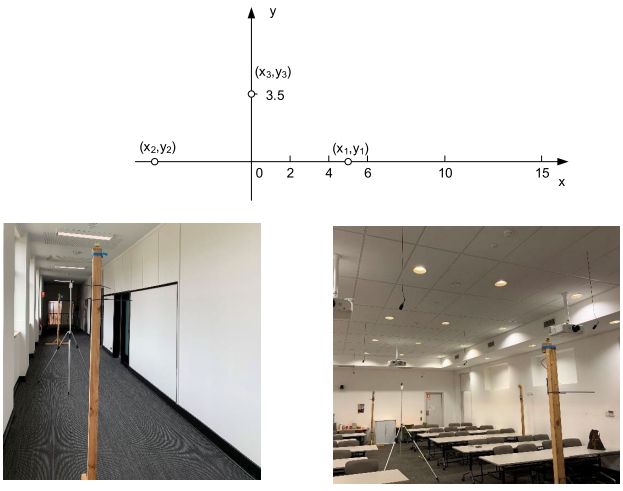

FIGURE 15. Setup of the two tests. For the 2D test (bottom left), two base stations were located at (x_1, y_1) and (x_2, y_2), and the mobile station was located at $(x, 0)$, x=0, 2, 4, 6, 10 and 15m. For the 3D test, one more base station was located at (x_3, y_3) as using TOA measurements only for 3D positioning requires at least three base stations, and the mobile station was located at $(0, 0, z)$ where z=0.18, 1.38 and 2.23m.

x-y plane where the base stations are located, the positioning error is getting smaller – mainly in the z direction. The HDOP values are very similar. The GDOP values at the three different locations i.e. (0,0,2.22), (0,0,1.38) and (0,0,0.18) are 353, 4.5 and 2.6 respectively. Note the (0,0,2.22) rather than (0,0,2.23) were used to calculate the GDOP to avoid infinity. When TOA was combined with AOA and only two base stations i.e. (x_1, y_1) and (x_2, y_2) were used, the GDOP values at (0,0,2.23), (0,0,1.38) and (0,0,0.18) are 2.60, 2.54, 2.37 respectively. Clearly, the GDOP decreased, and the user does not need to consider the height differences between the mobile station and the base stations. Fig. 17 (right) shows the positioning results are improved.

According to both the derived formula and the experiments, a few general rules can be summarized when base stations are deployed for hybrid AOA/TOA positioning:

- Adding a new AOA or TOA measurement will always decrease the DOP value. Deploying new stations can always achieve better DOP. Hence a convenient way to

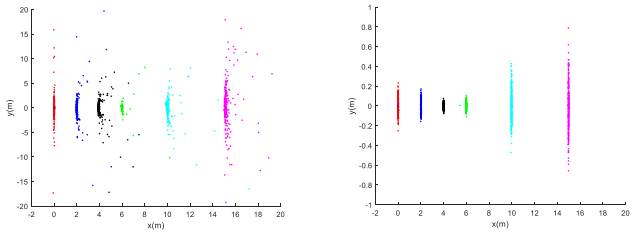

FIGURE 16. 2D test results: TOA only (left) vs. TOA+AOA (right).

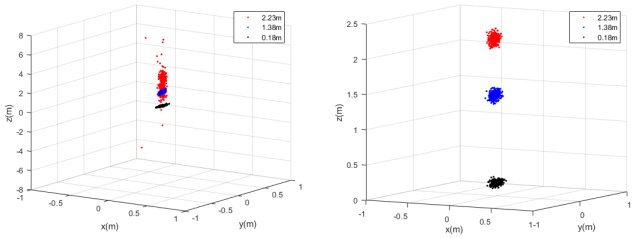

FIGURE 17. Positioning results in 3D scenario: TOA only (left, three base stations were used) vs. TOA+AOA (right, only two base stations on the *x* axis were used).

improve the accuracy is to add new stations to those areas in which the DOP values are relatively poor. This would not have negative influence on the nearby areas.

- Consider a circle centerd around a base station, a TOA measurement can improve the DOP along the radial direction while an AOA measurement can improve the DOP along the tangential direction. This explains why users do not need to consider the height differences between the mobile station and the base stations in 3D positioning when the TOA/AOA hybrid system is used.
- AOA measurements can significantly improve the DOP near a station while the TOA measurements improve the DOP evenly over the station's coverage area. The density of the base stations in an environment is related to both the accuracy of the AOA measurements and the range of the TOA measurements.

VII. FURTHER DISCUSSION OF THE DOP FOR AOA/TOA

In section V, it was demonstrated that changing the value of R (scaling up/down the size of the deployment) will change the DOP. This section discusses the range of DOP values of AOA/TOA and the proof is provided.

Property: Assuming there are enough AOA and TOA measurements for positioning independently (i.e. using AOA or TOA alone can estimate the position), the DOP value of AOA/TOA is less than that of either AOA or TOA. The DOP value approaches that of TOA only when R approaches infinity and it approaches that of AOA only when R approaches infinitely small.

Proof: Let us use the 3D scenario as an example (the base stations and the mobile station are not in the same plane, i.e. the height of the mobile station is different from the heights of the base stations) and $n \geq 3$. The A matrix (41) can be rewritten as:

$$A = \begin{bmatrix} a_{1,1} & a_{1,2} & a_{1,3} \\ & \cdots & \\ a_{n,1} & a_{n,2} & a_{n,3} \\ a_{(n+1),1} & a_{(n+1),2} & a_{(n+1),3} \\ & \cdots & \\ a_{2n,1} & a_{2n,2} & a_{2n,3} \\ a_{(2n+1),1} & a_{(2n+1),2} & a_{(2n+1),3} \\ & \cdots & \\ a_{3n,1} & a_{3n,2} & a_{3n,3} \end{bmatrix} \tag{46}$$

The covariance matrix of the position result can be expressed as:

$$cov(dp) = \begin{bmatrix} \sum_{i=1}^{3n} \frac{a_{i,1}a_{i,1}}{g(i)} & \sum_{i=1}^{3n} \frac{a_{i,1}a_{i,2}}{g(i)} & \sum_{i=1}^{3n} \frac{a_{i,1}a_{i,3}}{g(i)} \\ \sum_{i=1}^{3n} \frac{a_{i,2}a_{i,1}}{g(i)} & \sum_{i=1}^{3n} \frac{a_{i,2}a_{i,2}}{g(i)} & \sum_{i=1}^{3n} \frac{a_{i,2}a_{i,3}}{g(i)} \\ \sum_{i=1}^{3n} \frac{a_{i,3}a_{i,1}}{g(i)} & \sum_{i=1}^{3n} \frac{a_{i,3}a_{i,2}}{g(i)} & \sum_{i=1}^{3n} \frac{a_{i,3}a_{i,3}}{g(i)} \end{bmatrix}^{-1}$$

$$where\ g(i) = \begin{cases} {\sigma_\varphi}^2 & i \geq 1 \& i \leq n \\ {\sigma_\theta}^2 & i \geq n+1 \& i \leq 2n \\ {\sigma_r}^2 & i \geq 2n+1 \& i \leq 3n \end{cases} \tag{47}$$

It can be seen that when the deployment scales up (R increases), $a_{i,j}(i = 2n+1, 2n+2, \cdots, 3n; j = 1, 2, 3)$ remains the same as the numerator and the denominator increases proportionally (refer to (41)) while $a_{i,j}(i = 1, 2, \cdots, 2n; j = 1, 2, 3)$ becomes smaller as the value of the denominator increases faster than that of the numerator. When R approaches infinity, $a_{i,j}(i = 1, 2, \cdots, 2n; j = 1, 2, 3)$ approaches zero. Therefore, the first $2n$ terms of each element in (47) can be ignored. If only the range measurements are used for positioning, the A matrix can be expressed as:

$$A_{TOA} = \begin{bmatrix} \frac{x-x_1}{u_1} & \frac{y-y_1}{u_1} & \frac{z-z_1}{u_1} \\ & \cdots & \\ \frac{x-x_n}{u_n} & \frac{y-y_n}{u_n} & \frac{z-z_n}{u_n} \end{bmatrix} = \begin{bmatrix} a_{(2n+1),1} & a_{(2n+1),2} & a_{(2n+1),3} \\ & \cdots & \\ a_{3n,1} & a_{3n,2} & a_{3n,3} \end{bmatrix} \tag{48}$$

And the covariance can be expressed as:

$$cov(dp) = \begin{bmatrix} \sum_{i=2n+1}^{3n} \frac{a_{i,1}a_{i,1}}{{\sigma_r}^2} & \sum_{i=2n+1}^{3n} \frac{a_{i,1}a_{i,2}}{{\sigma_r}^2} & \sum_{i=2n+1}^{3n} \frac{a_{i,1}a_{i,3}}{{\sigma_r}^2} \\ \sum_{i=2n+1}^{3n} \frac{a_{i,2}a_{i,1}}{{\sigma_r}^2} & \sum_{i=2n+1}^{3n} \frac{a_{i,2}a_{i,2}}{{\sigma_r}^2} & \sum_{i=2n+1}^{3n} \frac{a_{i,2}a_{i,3}}{{\sigma_r}^2} \\ \sum_{i=2n+1}^{3n} \frac{a_{i,3}a_{i,1}}{{\sigma_r}^2} & \sum_{i=2n+1}^{3n} \frac{a_{i,3}a_{i,2}}{{\sigma_r}^2} & \sum_{i=2n+1}^{3n} \frac{a_{i,3}a_{i,3}}{{\sigma_r}^2} \end{bmatrix}^{-1} \tag{49}$$

When the first $2n$ terms of each element in (47) are ignored, (47) is exactly the same as (49). Hence, the DOP value of the AOA/TOA combined system is the same as that of the TOA only system.

On the contrary, when the deployment scales down (R decreases), $a_{i,j}(i = 2n+1, 2n+2, \cdots, 3n; j = 1, 2, 3)$ remains the same while $a_{i,j}(i = 1, 2, \cdots, 2n; j = 1, 2, 3)$ becomes larger as the value of the denominator decreases faster than that of the numerator. When R approaches 0, $a_{i,j}(i = 1, 2, \cdots, 2n; j = 1, 2)$ approaches infinity or negative infinity ($a_{i,3}(i = 1, 2, \cdots, 2n)$ are zeros). Then the last n terms of each element can be ignored. Hence the DOP value of the AOA/TOA combined system is the same as that of the AOA only system.

The parameter k also has an impact on the DOP value. When changing the k value, the impact on DOP is similar to that of changing the R value but in the opposite way, i.e. increasing k is equivalent to decreasing R and vice versa. The details are not discussed here.

VIII. CONCLUSION

For a range and/or angle measurement based positioning system, the positioning accuracy is affected by the geometric distribution of the base stations. DOP is a value that can describe the effect on the relationship between measurement error and position determination error. The DOP of the TOA system or the AOA system has been investigated separately before. In this article, the DOP of a positioning system combining TOA and AOA measurements has been investigated under different scenarios (2D or 3D). Unified formulae have been derived and the DOP values of several different deployments of base stations have been examined. It has been shown that the DOP value is related to the size of the deployment of the system. When the size of the deployment scales up to infinity, the DOP is decided by the TOA part of the system, but when the size scales down to infinitely small, the DOP is decided by the AOA part of the system. As more AOA based positioning systems are being developed, a combined system using AOA and TOA (or TDOA) is likely to be widely used in the near future. The DOP of the combined system can help to guide the deployment of the base stations.

REFERENCES

[1] R. F. Brena, J. P. García-Vázquez, C. E. Galván-Tejada, D. Muñoz-Rodriguez, C. Vargas-Rosales, and J. Fangmeyer, "Evolution of indoor positioning technologies: A survey," *J. Sensors*, vol. 2017, Mar. 2017, Art. no. 2630413.

[2] C. Hide, T. Botterill, and M. Andreotti, "Low cost vision-aided IMU for pedestrian navigation," in *Proc. Ubiquitous Positioning Indoor Navigat. Location Based Service*, Oct. 2010, pp. 1–7.

[3] B. Li, A. G. Dempster, J. Barnes, C. Rizos, and D. Li, "Probabilistic algorithm to support the fingerprinting method for CDMA location," in *Proc. Int. Symp. On GPS/GNSS*, 2005, pp. 8–10.

[4] B. Hofmann-Wellenhof, H. Lichtenegger, and J. Collins, *Global Positioning System: Theory and Practice*. Springer, 2012.

[5] J. V. Carroll and J. A. Weitzen, "GPS and loran-C: A great approach navigation system for general aviation aircraft," *GPS Solutions*, vol. 1, no. 1, pp. 11–12, Jul. 1995.

[6] C. Mensing and S. Plass, "Positioning algorithms for cellular networks using TDOA," in *Proc. IEEE Int. Conf. Acoust. Speed Signal Process.*, May 2006, pp. IV–IV.

[7] C. Rizos, G. Roberts, J. Barnes, and N. Gambale, "Experimental results of locata: A high accuracy indoor positioning system," in *Proc. Int. Conf. Indoor Positioning Indoor Navigat.*, Sep. 2010, pp. 1–7.

[8] R. Peng and M. L. Sichitiu, "Angle of arrival localization for wireless sensor networks," in *Proc. 3rd Annu. IEEE Commun. Soc. Sensor Ad Hoc Commun. Netw.*, Sep. 2006, pp. 374–382.

[9] M. Samimi, K. Wang, Y. Azar, G. N. Wong, R. Mayzus, H. Zhao, J. K. Schulz, S. Sun, F. Gutierrez, and T. S. Rappaport, "28 GHz angle of arrival and angle of departure analysis for outdoor cellular communications using steerable beam antennas in new york city," in *Proc. IEEE 77th Veh. Technol. Conf. (VTC Spring)*, Jun. 2013, pp. 1–6.

[10] Y. Zhou, C. L. Law, Y. L. Guan, and F. Chin, "Indoor elliptical localization based on asynchronous UWB range measurement," *IEEE Trans. Instrum. Meas.*, vol. 60, no. 1, pp. 248–257, Jan. 2011.

[11] S. Shin, M.-H. Kim, and S. B. Choi, "Ultrasonic distance measurement method with crosstalk rejection at high measurement rate," *IEEE Trans. Instrum. Meas.*, vol. 68, no. 4, pp. 972–979, Apr. 2019.

[12] F. H. Moffitt and J. D. Bossler, *Surveying*, 10th ed. Menlo Park, CA, USA, Addison-Wesley, 1998.

[13] H.-C. Chen, T.-H. Lin, H. T. Kung, C.-K. Lin, and Y. Gwon, "Determining RF angle of arrival using COTS antenna arrays: A field evaluation," in *Proc. IEEE Mil. Commun. Conf. (MILCOM)*, Oct. 2012, pp. 1–6.

[14] S.-F. Chuang, W.-R. Wu, and Y.-T. Liu, "High-resolution AoA estimation for hybrid antenna arrays," *IEEE Trans. Antennas Propag.*, vol. 63, no. 7, pp. 2955–2968, Jul. 2015.

[15] S. Wielandt, J.-P. Goemaere, and L. De Strycker, "2.4 GHz synthetic linear antenna array for indoor propagation measurements in static environments," in *Proc. Int. Conf. Indoor Positioning Indoor Navigat. (IPIN)*, Alcalá de Henares, Spain, 2016, pp. 4–7.

[16] M. Schüssel, "Angle of arrival estimation using WiFi and smartphones," in *Proc. Int. Conf. Indoor Positioning Indoor Navigat. (IPIN)*, vol. 4, 2016, p. 7.

[17] A. Kangas and T. Wigren, "Angle of arrival localization in LTE using MIMO pre-coder index feedback," *IEEE Commun. Lett.*, vol. 17, no. 8, pp. 1584–1587, 2013.

[18] S. Bluetooth, "Enhancing Bluetooth location services with direction finding," Bluetooth Special Interest Group, Kirkland, WA, USA, Tech. Rep., vol. 1, 2019. https://3pl46c46ctx02p7rzdsvsg21-wpengine.netdna-ssl.com/wp-content/upl% oads/2019/03/1901_Enhancing-Bluetooth-Location-Service_FINAL.pdf

[19] J. Kasper and C. Hutchinson, "The omega navigation system–An overview," *IEEE Commun. Soc. Mag.*, vol. 16, no. 3, pp. 23–35, May 1978.

[20] Z. Sahinoglu, S. Gezici, and I. Guvenc, *Ultra-Wideband Positioning Systems*. New York, NY, USA: Cambridge, 2008.

[21] X. Lv, K. Liu, and P. Hu, "Geometry influence on GDOP in TOA and AOA positioning systems," in *Proc. 2nd Int. Conf. Netw. Secur., Wireless Commun. Trusted Comput.*, 2010, pp. 58–61.

[22] B. Li, A. G. Dempster, and J. Wang, "3D DOPs for positioning applications using range measurements," *Wireless Sensor Netw.*, vol. 3, no. 10, p. 334, 2011.

[23] W. Shi, X. Qi, J. Li, S. Yan, L. Chen, Y. Yu, and X. Feng, "Simple solution to the optimal deployment of cooperative nodes in two-dimensional TOA-based and AOA-based localization system," *EURASIP J. Wireless Commun. Netw.*, vol. 2017, no. 1, p. 79, Dec. 2017.

[24] D. H. Won, J. Ahn, S.-W. Lee, J. Lee, S. Sung, H.-W. Park, J.-P. Park, and Y. J. Lee, "Weighted DOP with consideration on elevation-dependent range errors of GNSS satellites," *IEEE Trans. Instrum. Meas.*, vol. 61, no. 12, pp. 3241–3250, Dec. 2012.

[25] M. H. Bergen, F. S. Schaal, R. Klukas, J. Cheng, and J. F. Holzman, "Toward the implementation of a universal angle-based optical indoor positioning system," *Frontiers Optoelectron.*, vol. 11, no. 2, pp. 116–127, Jun. 2018.

[26] A. G. Dempster, "Dilution of precision in angle-of-arrival positioning systems," *Electron. Lett.*, vol. 42, no. 5, pp. 291–292, Mar. 2006.

[27] Y.-Y. Li, G.-Q. Qi, and A.-D. Sheng, "Performance metric on the best achievable accuracy for hybrid TOA/AOA target localization," *IEEE Commun. Lett.*, vol. 22, no. 7, pp. 1474–1477, Jul. 2018.

[28] N. Levanon, "Lowest GDOP in 2-D scenarios," *IEE Proc.-Radar, Sonar Navigat.*, vol. 147, no. 3, pp. 149–155, Jun. 2000.

[29] H. Lee, "A novel procedure for assessing the accuracy of hyperbolic multilateration systems," *IEEE Trans. Aerosp. Electron. Syst.*, vol. AES-11, no. 1, pp. 2–15, Jan. 1975.

[30] X. Zhang, L. Xu, L. Xu, and D. Xu, "Direction of departure (DOD) and direction of arrival (DOA) estimation in MIMO radar with reduced-dimension MUSIC," *IEEE Commun. Lett.*, vol. 14, no. 12, pp. 1161–1163, Dec. 2010.

[31] Decawave. (2017). *Dw1000 User Manual*. https://www.decawave.com/sites/default/files/resources/dw1000_user_manu% al_2.11.pdf

BINGHAO LI (Member, IEEE) received the B.E. degree in electrical and mechanical engineering from Beijing Jiaotong University, China, in 1994, the M.E. degree in civil engineering from Tsinghua University, China, in 2001, and the Ph.D. degree from the University of New South Wales at Sydney, Sydney, Australia, in 2006. He is currently a Senior Lecturer with the School of Minerals and Energy Resources Engineering, University of New South Wales at Sydney. His research interests include indoor positioning, pedestrian navigation, satellite positioning and navigation, and the mine Internet of Things.

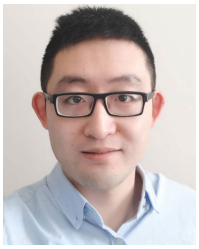

KAI ZHAO received the B.E. degree from Tsinghua University, in 2011, and the M.E. degree from the University of New South Wales at Sydney, in 2014. He is currently a Research Assistant with the University of New South Wales at Sydney. He has extensive experience in the IoT and wireless device development. His research interests include ultra-wide-band, sensor fusion, indoor positioning, and their applications.

XUESONG SHEN is currently a Senior Lecturer of engineering construction and management and the Founder and Director of the Autonomy and Intelligence in Construction Laboratory (AICON), School of Civil and Environmental Engineering, University of New South Wales (UNSW) at Sydney, Sydney, Australia. His research interests include autonomous systems, artificial intelligence, digital twins, smart sensing, the Internet of Things, mixed reality, and their applications in the preparation, construction, operation, and maintenance of civil infrastructure and the built environment. He represents Australia in the Board of Directors of the prestigious International Association for Automation and Robotics in Construction (IAARC).